Influence of tether dynamics on forced Kramers escape from a kinetic trap

Anirban Sain[1,*] and Michael Wortis[2]
[1]*Physics Department, McGill University, Rutherford Building, 3600 rue University, Montreal, Quebec, Canada H3A 2T8*
[2]*Department of Physics, Simon Fraser University, Burnaby, British Columbia, Canada V5A 1S6*
(Received 16 March 2004; published 3 September 2004)

When a trapped particle is subject to the tension of a massive frictional spring (the "tether"), the escape rate increases due to a lowering of the escape barrier. However, in addition, the escape-rate prefactor is influenced by the mass and drag contributed by the spring. We solve the full Kramers escape problem for the coupled system using a technique attributed to Langer. The prefactor in the escape rate is significantly modified by the spring parameters even in the strong-damping limit. The biophysical relevance of this problem is briefly discussed.

DOI: 10.1103/PhysRevE.70.031102 PACS number(s): 82.20.Uv, 82.39.−k, 02.50.Ey, 05.40.−a

I. INTRODUCTION

In 1940 Kramers [1] solved the problem of the escape rate of a particle trapped in a metastable state by the potential $V(X)$ (a "kinetic trap") and subject to thermal noise and a damping force. The equation of motion of the particle was given by

$$M\ddot{X} = -\gamma_M M\dot{X} - \frac{dV}{dX} + \eta(t), \tag{1}$$

with a Gaussian white noise satisfying

$$\langle \eta(t)\,\eta(t')\rangle = 2\gamma_M M k_B T \delta(t-t'), \tag{2}$$

in order that the system achieve thermal equilibrium at temperature T. Kramers' result for the escape rate can be written

$$r_{Kr} = \frac{\lambda_+^{Kr}}{2\pi} R_{Kr} e^{-Q/k_B T}. \tag{3}$$

In Eq. (3) $R_{Kr}=\omega_s/\omega_u$ is a ratio of frequencies associated with the curvature of the potential function at the metastable (s) and unstable (u) equilibrium points via $M\omega_{s,u}^2 \equiv \pm V''_{s,u}$. The factor

$$\lambda_+^{Kr} = \frac{1}{2}(\sqrt{\gamma_M^2 + 4\omega_u^2} - \gamma_M) = \frac{1}{2}\left[\sqrt{\left(\frac{\Gamma_M}{M}\right)^2 + 4\frac{|V''_u|}{M}} - \frac{\Gamma_M}{M}\right], \tag{4}$$

carries the dependence on the particle mass M and the drag coefficient γ_M per unit mass (alternatively, $\Gamma_M \equiv M\gamma_M$ is the net drag coefficient). And, Q is the energy barrier for escape. As a function of γ_M, the factor λ_+ decreases monotonically from ω_u at $\gamma_M=0$ to ω_u^2/γ_M as $\gamma_M\to\infty$, illustrating how increasing the drag per unit mass reduces the escape rate [2]. In terms of the variables M, Γ_M, the Kramers escape rate varies as $1/\sqrt{M}$ for $\Gamma_M\to 0$ (M fixed) and as $1/\Gamma_M$ for $\Gamma_M\to\infty$ (independent of mass). The derivation of Eq. (3) assumes that Q/k_BT is appreciably greater than unity, so that escape is slow enough to be independent of initial conditions, and

$$\gamma_M > \omega_s \frac{k_B T}{Q}, \tag{5}$$

which expresses the requirement that the dissipative energy loss per cycle be larger than k_BT.

An additional fixed force F applied to M in such a direction as to pull it out of the trap may be expected to increase the escape rate. We shall refer to this situation as "forced" escape. Such a force may be represented by modifying the potential according to $V(X)\to E_0(X)=V(X)+FX$ (the sign has been chosen so that the particle escapes towards lower values of X). This addition changes the equilibrium positions. Thus, the barrier height

$$Q_{forced} = [V(X_u) - V(X_s)] - F(X_s - X_u), \tag{6}$$

is reduced from the unforced case because of the shifts in equilibrium positions and also because of the explicit force term, both of which make escape more rapid, as was emphasized originally by Bell [3] and more recently by Evans and Ritchie [4]. Of course, the frequencies $\omega_{s,u}$ are also modified, because of the change in the equilibrium points, but this effect is usually of secondary importance. With these modifications, the Kramers equations (3) and (4) remain valid for the forced escape.

The purpose of this article is to explore how the forced-Kramers escape rate is modified when the force is applied by a massive frictional polymeric spring or "tether" rather than by a simple linear potential.

This question is motivated by recent biophysical experiments [5,6] in which noncovalent bonds are broken by the application of an external force. Typically, the force (in the pico-newton range) is applied by a soft cantilever coupled to the bonding region via a polymeric linker. Linker molecules include DNA, polysaccharides, parts of the muscle protein titin [5–8], etc. The force is slowly increased until bond rupture occurs. In a purely mechanical problem, rupture would occur when the applied force reaches the maximum slope of the trapping potential. However, in the presence of a thermal bath, rupture is a statistical process that can occur well before the mechanical rupture point, provided time is available

*Present address: Physics Department, Indian Institute of Technology Bombay, Powai, Mumbai-400 076, India.

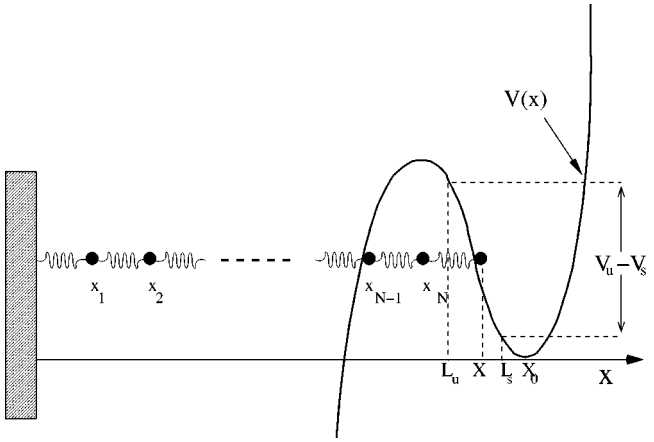

FIG. 1. The polymeric spring consists of N coupled masses, situated at the points $x_1, x_2, \ldots x_N$, attached at one end to a fixed wall ($x=0$) and at the other end to the trapped mass M at $x=X \equiv x_{N+1}$. The tension in the spring shifts the metastable equilibrium leftward from X_0 to L_s and the unstable equilibrium rightward from the top of the escape barrier to L_u. The spring tension is adjusted by rigidly shifting the position X_0 of the potential minimum. When tension is present, the barrier height Q is given by Eq. (32).

for a sufficiently energetic fluctuation to become available. In this sense, thermally assisted rupture becomes equivalent to forced escape from a kinetic trap. Rather than a single rupture strength, experiments measure a spectrum of such strengths. In an important article, Evans and Ritchie [4] have explained how such spectra are to be interpreted. In particular, they stress the importance of the rate at which the applied force is ramped up prior to rupture. If the ramping rate is very rapid (the mechanical limit), then no time is available for thermal fluctuations and the spectrum of rupture strengths approaches the mechanical value. If, on the other hand, the ramping rate is very slow (the thermal limit), then thermal fluctuations are important, and escape (rupture) can occur with low or zero force. Typical experiments [5,6] probe the region between these limits. Our calculations will address the escape rate at fixed force, not the influence of the ramping rate.

Our objective is to explore in the simplest possible context how the mass and drag of the polymeric linker influences the escape rate. The model we shall treat, a one-dimensional mass-and-spring enthalpic polymer, is introduced in Sec. II. In Sec. III we use a method attributed to Langer [9] to write down an escape rate and show how that rate reduces to known results in simple limits. Section IV uses a variety of examples to illustrate the dependence of the escape rate on the polymeric properties. Section V provides brief additional discussion.

II. MODEL: MECHANICS

The system we consider is a mass-and-spring polymer coupled to a trapping potential $V(X)$ which is centered about the position X_0 (see Fig. 1). The polymer consists of N point masses m coupled by harmonic springs, each of equilibrium length a. At one end, the polymer is attached to a fixed wall by an initial spring; at the other end, it is attached via a terminal spring to a mass M at position $X \equiv x_{N+1}$ which is subject to the trapping potential. All motion is in one dimension. For simplicity we take all springs to be equivalent. In the absence of dissipation, the potential energy of this system is

$$E = \frac{k}{2}[(x_1 - a)^2 + (x_2 - x_1 - a)^2 + \cdots + (X - x_N - a)^2] + V(X). \tag{7}$$

When unstretched, the total length of the polymer (including the end springs) is $L_0=(N+1)a$. We have placed the minimum of the potential at a position $X_0 > L_0$, so that, as long as X is in the region of the trapping potential, the polymeric spring is always under tension. Thus, the stable (s) equilibrium position of the trapped particle is displaced leftward from the potential minimum to the position L_s with $L_0 < L_s < X_0$, while the unstable (u) equilibrium position is displaced to the right from the lip of the potential to the position L_u with $L_0 < L_u < L_s$. Of course, if X_0 is too large, $X_0 > X_0^{max}$, then the stable and unstable equilibrium points merge and disappear, as the polymeric tension overcomes the trapping potential. We focus on the situation $X_0 < X_0^{max}$, where there is a stable trap with $L_s - L_u$ comparable to the molecular scale a.

When the system is at equilibrium (either stable or unstable), the springs are all stretched by the same amount, so

$$X = L \equiv (N+1)l \quad \text{and} \quad x_n = nl, \;\; n = 1, \ldots, N. \tag{8}$$

Under these conditions, the polymeric tension is

$$F = k(l-a) = ka\left[\frac{L - L_0}{L_0}\right] = Y_0 \frac{\Delta L}{L_0}, \tag{9}$$

which identifies Young's modulus of the polymer as

$$Y_0 = ka = \frac{k}{(N+1)} L_0. \tag{10}$$

Substituting (8) into (7), we find the energy of the uniformly stretched system

$$E_0(X) = \frac{1}{2}\frac{Y_0}{L_0}(X - L_0)^2 + V(X). \tag{11}$$

Thus, at equilibrium (stable or unstable) $-dV/dX|_{X=L_{s,u}} = F = Y_0[(L_{s,u} - L_0)/L_0]$, which determines L in terms of X_0 and L_0. Equilibrium is stable (unstable) according to $d^2E_0/dX^2|_L = (Y_0/L_0) + V'' > 0 (< 0)$. Thus, at the unstable equilibrium $V_u'' < 0$ with $|V_u''| > Y_0/L_0$, so

$$0 < \alpha \equiv \frac{Y_0}{L_0|V_u''|} < 1. \tag{12}$$

It will from time to time be useful to have in mind the specific model potential

$$V(X) = \frac{K_1}{2}(X - X_0)^2 + \frac{K_2}{3}(X - X_0)^3. \tag{13}$$

The condition that the scale of the potential should be of order a requires $K_1/K_2 \sim a$. For this potential, it is easy to verify that

$$L_{s,u} = X_0 - \frac{1}{2K_2}\left(K_1 + \frac{Y_0}{L_0}\right) \pm \frac{1}{2K_2}\sqrt{\left(K_1 + \frac{Y_0}{L_0}\right)^2 - 4K_2Y_0\left(\frac{X_0 - L_0}{L_0}\right)}, \tag{14}$$

from which

$$X_0^{max} = L_0 + \frac{L_0}{4K_2Y_0}\left(K_1 + \frac{Y}{L_0}\right)^2. \tag{15}$$

Finally, we note for future reference that the second derivative of the potential evaluated at the equilibrium points is

$$V''_{s,u} \equiv \left.\frac{d^2V}{dX^2}\right|_{s,u} = \pm\sqrt{\left(K_1 + \frac{Y_0}{L_0}\right)^2 - 4K_2Y_0\left(\frac{X_0 - L_0}{L_0}\right)} - \frac{Y_0}{L_0}. \tag{16}$$

To describe motion near either one of the equilibrium states (s,u), it is convenient to introduce variables

$$u_n \equiv x_n - nl_{s,u}, \quad n = 1, \ldots, N+1, \tag{17}$$

and then to expand the potential energy about equilibrium

$$E^{(s,u)}(\{u_n\}) = E_0^{(s,u)} + \tfrac{1}{2}\mathbf{u}^{\mathbf{T}}\mathbf{E}_{\mathbf{2}}^{(\mathbf{s},\mathbf{u})}\mathbf{u} + \cdots, \tag{18}$$

where

$$E_0^{(s,u)} = E_0(L_{s,u}) = \frac{1}{2}\frac{Y_0}{L_0}(L_{s,u} - L_0)^2 + V_{s,u}, \tag{19}$$

and $\mathbf{E}_{\mathbf{2}}^{(\mathbf{s},\mathbf{u})}$ is the matrix of second derivatives of (7) evaluated at the appropriate equilibrium point. This leads to equations of motion linearized about equilibrium

$$\begin{aligned}
m\partial_t^2 u_1 &= -m\gamma\partial_t u_1 - k(2u_1 - u_2) + \eta_1 \\
m\partial_t^2 u_2 &= -m\gamma\partial_t u_2 - k(2u_2 - u_1 - u_3) + \eta_2 \\
&\cdots \\
m\partial_t^2 u_N &= -m\gamma\partial_t u_N - k(2u_N - u_{N-1} - u_{N+1}) + \eta_N \\
M\partial_t^2 u_{N+1} &= -M\gamma_M\partial_t u_{N+1} - k(u_{N+1} - u_N) - V''u_{N+1} + \eta_{N+1},
\end{aligned} \tag{20}$$

where we have introduced a velocity-dependent damping force, which may be different for the trapped and polymeric masses. The terms $\eta_m(t)$ represent a set of independent Gaussian random forces satisfying the usual conditions

$$\begin{aligned}
\langle \eta_m(t)\,\eta_n(t')\rangle &= 2m\gamma k_B T\delta_{mn}\delta(t - t') \\
&\quad \text{for } m,\ n = 1, \ldots, N+1 \\
&\quad \text{except that } \langle \eta_{N+1}(t)\,\eta_{N+1}(t')\rangle \\
&= 2M\gamma_M k_B T\delta(t - t'),
\end{aligned} \tag{21}$$

which ensures that the system reaches thermal equilibrium at temperature T [10].

It will be convenient in what follows to consider the continuum limit of the polymer, where N and k go to infinity and a, l, and m go to zero in such a way that L_0, L, Y_0, and the polymer mass per unit length $\mu \equiv m/l$ remain fixed. Taking this limit in Eqs. (20), we replace the discretely indexed set $\{u_n(t)\}$ by the continuous function $u(x,t)$ with $x = nl \in [0,L]$. This process leads to a damped (longitudinal) wave equation

$$\mu(\partial_t^2 u + \gamma\partial_t u) = Y\partial_x^2 u, \tag{22}$$

along with the boundary conditions

$$u(0,t) = 0 \quad \text{and} \quad M\left(\partial_t^2 u + \gamma_M\partial_t u + \frac{V''}{M}u\right)\Bigg|_{x=L} = -Y\partial_x u|_{x=L}, \tag{23}$$

where

$$\frac{Y}{L} \equiv \frac{Y_0}{L_0} = \frac{F + Y_0}{L}, \tag{24}$$

and the noise terms have been dropped [11].

Equations (22) and (23) are a linear system, and it is straightforward to do the normal-mode analysis. If the normal mode is written $u(x,t) = h(x)e^{\lambda t}$, then eigenfunctions $h(x)$ satisfying the boundary condition at $x = 0$ have the form $\sin qx$ or $\sinh qx$. Corresponding eigenvalues obey $\lambda^2 + \gamma\lambda = \mp(Y/\mu)q^2$ for the $\sin qx$ (upper sign) and $\sinh qx$ (lower sign), respectively. The boundary condition at $x = L$ then selects allowed q values (if any). In Sec. III we will need the (unique) unstable (i.e., positive real) eigenvalue λ_+ associated with the unstable equilibrium. It is easy to show that this eigenvalue can only arise from a solution of the $\sinh qx$ type. It is useful to define

$$z \equiv qL, \quad \omega_\mu^2 \equiv \frac{Y}{\mu L^2}, \quad \omega_M^2 \equiv \frac{Y}{ML}, \tag{25}$$

and the dimensionless ratios

$$\alpha \equiv \frac{\omega_M^2}{\omega_u^2} = \frac{Y}{L|V''_u|} \quad \text{and} \quad \beta \equiv \frac{\omega_\mu^2}{\omega_M^2} = \frac{M}{\mu L}. \tag{26}$$

In terms of these variables, the eigenvalue obeys

$$\lambda_+^2 + \gamma\lambda_+ = \omega_\mu^2 z^2, \tag{27}$$

with solution

$$\lambda_+(z) = \tfrac{1}{2}\left(\sqrt{\gamma^2 + 4\omega_\mu^2 z^2} - \gamma\right) = \tfrac{1}{2}\left(\sqrt{\gamma^2 + 4\alpha\beta\omega_u^2 z^2} - \gamma\right). \tag{28}$$

In order to satisfy the boundary condition (23) at $x = L$, z must be chosen to solve

$$\tanh z = \frac{\omega_M^2 z}{\omega_u^2 - [\lambda_+^2(z) + \gamma_M \lambda_+(z)]}. \tag{29}$$

To find the eigenvalue λ_+, it is necessary to solve (29) simultaneously with (27) or (28). We shall use these equations as our starting point in Sec. III.

III. STATISTICAL MECHANICS: ESCAPE RATE

The escape rate for problems of the general type (7) was originally worked out by Langer [9,12]. As noted by Hänggi *et al.* [12], the Langer result is just the multidimensional generalization of the original Kramers rate [1]. Like the Kramers result, it may be viewed as the result of solving the full Fokker-Planck equation at the harmonic level in the barrier region and coupling this solution to appropriate boundary conditions inside and outside the trap. In the notation of our article, Langer's escape rate can be written

$$r = \frac{\lambda_+}{2\pi} R e^{-Q/k_B T}, \tag{30}$$

in strict parallel with the Kramers result (3), only now λ_+ is the eigenvalue [11] defined by Eqs. (28) and (29)

$$R \equiv \left| \frac{\det \mathbf{E_2}^{(s)}}{\det \mathbf{E_2}^{(u)}} \right|^{1/2}, \tag{31}$$

and

$$Q = E_0^{(u)} - E_0^{(s)} = V_u - V_s + \frac{1}{2}\frac{Y_0}{L_0}[(L_u - L_0)^2 - (L_s - L_0)^2] \tag{32}$$

is the energy difference between the unstable and stable equilibrium configurations. The ratio of determinants can be evaluated exactly (see the Appendix)

$$R = \left[\frac{V_s'' + Y/L}{|V_u''| - Y/L}\right]^{1/2} = \left[\frac{\omega_s^2 + \omega_M^2}{\omega_u^2 - \omega_M^2}\right]^{1/2} = \frac{1}{\omega_u}\left[\frac{\omega_s^2 + \omega_M^2}{1-\alpha}\right]^{1/2}. \tag{33}$$

The final result in the continuum limit is

$$r = \frac{1}{4\pi}(\sqrt{\gamma^2 + 4\omega_\mu^2 z^2} - \gamma)\left[\frac{V_s'' + Y/L}{|V_u''| - Y/L}\right]^{1/2} e^{-Q/k_B T}. \tag{34}$$

Like the original Kramers result (3), this expression is expected to fail if the damping γ becomes too small, a limitation we shall discuss further in Sec. V B.

Equation (34) gives the dependence of the escape rate on the properties of the polymeric link and is our central result. In what follows, we will explore the implications of this formula. We begin with a few general remarks. The ratio R defined by Eq. (33) is a straightforward generalization of R_{Kr}. The additional terms $Y/L = Y_0/L_0$ reflect the inclusion of the polymeric terms in the second derivatives of the full potential $E_0(X)$, Eq. (11). Note that R is mass independent. Furthermore, the denominator of Eq. (33) is necessarily positive by virtue of Eq. (12). Thus, in discussing the behavior of the escape rate, variations of R are not normally important. Indeed, for the model potential (13), Eq. (16) shows that $R = 1$. The polymeric tension, on the other hand, is important. Tension is adjusted by increasing or decreasing the offset X_0, which sets the lengths $L_{s,u}$, as illustrated by Eq. (14). These lengths enter the barrier height (32) both explicitly and implicitly via their effect on V_u and V_s. In the normal case, where the tension does not change significantly between the stable and unstable equilibrium points, the last term of (32) can be approximated by a simple product, $F(L_u - L_s)$, of the tension (9) and the displacement between stable and unstable equilibrium positions [cf. Eq. (6)]. Of course, as the tension increases towards the instability point [e.g., Eq. (15)], then L_u and L_s approach one another, as do V_u and V_s. Thus, the barrier Q shrinks and, at the same time, the denominator of (33) approaches zero, i.e., $\alpha \to 1^-$. Both these effects increase the escape rate dramatically [13]. In what follows, we shall assume that we are not near this instability, so that $Q \gg k_B T$ and α, which is always in the interval (12), is not close to unity. In this region, the exponential $e^{-Q/k_B T}$, although numerically important, is not particularly interesting. It is the factor λ_+ in (30) which incorporates the important interplay between the mass M and the attached polymer. This factor is the focus of our further analysis below.

The key issue in finding $\lambda_+(z)$ is solving Eq. (29) for z. By using Eq. (28), we rewrite (29) in the convenient form

$$\frac{\tanh z}{z} = \frac{\alpha}{D(z)}, \tag{35}$$

where the denominator is

$$D(z) = 1 - \alpha\beta z^2 + \frac{(\gamma - \gamma_M)}{2\omega_u}\left[\sqrt{\left(\frac{\gamma}{\omega_u}\right)^2 + 4\alpha\beta z^2} - \frac{\gamma}{\omega_u}\right]. \tag{36}$$

The left side of (35) has the value unity at $z = 0$ and decreases monotonically towards zero as z increases. It is easy to verify that $dD/dz < 0$ (for $\gamma_M \geqslant 0$), so $D(z)$ decreases smoothly from its initially positive value of unity at $z = 0$, passes through a unique zero at some z_0, and continues to negative values at large z. Thus, the right side of (35) increases monotonically from an initial value $\alpha < 1$, diverges at $z = z_0$, and continues at negative values. It follows that (35) always has a unique solution z with $0 < z < z_0$, as illustrated in Fig. 2. Note that, as long as α is not very small, then $z \sim 1$, unless $z_0 \ll 1$, in which case $z \sim z_0$. The case $\gamma = \gamma_M$ is especially transparent, since (35) takes the simple form

$$\frac{\tanh z}{z} = \frac{\alpha}{1 - \alpha\beta z^2}. \tag{37}$$

It is worth commenting on the scaling of the solutions. The original variables of Eqs. (27)–(29), ω_M, ω_u, ω_μ, γ, and γ_M, all have the same units. It follows that λ_+/ω_u depends on four dimensionless ratios of these five quantities, which we may take, for example, to be α, β, γ/ω_u, and γ_M/ω_u. The dependence of the escape rate on these four variables is in general nonsimple, as it is necessary to solve Eq. (35) for $z = z(\alpha, \beta, \gamma/\omega_u, \gamma_M/\omega_u)$ and then to substitute this into (28). Only in special cases is there a little simplification. One ex-

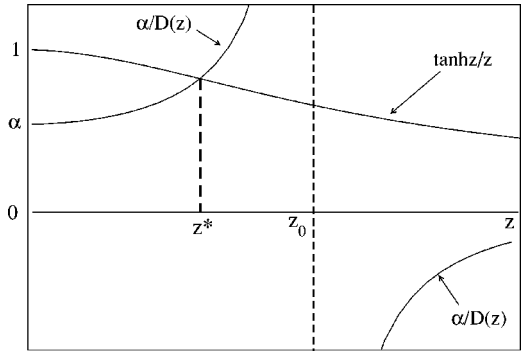

FIG. 2. Schematic graph of the left and right sides of Eq. (35). Because $\alpha<1$ and $D(z)$ vanishes at $z=z_0$, there is a unique positive solution $z=z^*$ in the interval $0<z<z_0$.

ample is that of Eq. (37), which is independent of γ so that $z=z(\alpha,\beta)$ and the full γ dependence can be read off from Eq. (28).

Certain important limiting results emerge immediately from the above framework, which we now discuss.

A. Original Kramers limit, $Y_0=Y=0$ ($\alpha=0$)

This corresponds to setting the spring constants k to zero, so that the polymer has no influence on the escape problem. Clearly, the original Kramers result (3) and (4) must reemerge. The R factors are simple, since $\omega_M^2=0$, so $R\rightarrow\omega_s/\omega_u=R_{Kr}$. The solution for λ_+ is a bit more complicated, since ω_μ^2 also vanishes but in such a way that the product $\omega_\mu^2 z^2$ remains finite. The key is to notice that, under these conditions, the solution occurs for $z\gg 1$, so $\tanh z\approx 1$, and (35) reduces to the condition $D(z)=0$. A few lines of algebra show that this condition is equivalent to

$$\sqrt{\gamma^2+4\omega_\mu^2 z^2}-\gamma=\sqrt{\gamma_M^2+4\omega_\mu^2}-\gamma_M, \tag{38}$$

so that $\lambda_+\rightarrow\lambda_+^{Kr}$, reproducing (4).

B. "Forced"-Kramers limit, $\mu=0$ (γ fixed)

Taking the mass of the polymer to zero also eliminates the polymeric drag; however, the tension of the polymer remains, thus converting the original potential $V(X)$ to the modified potential $E_0(X)$, Eq. (11). When this potential is treated by the Kramers formula, the result is

$$r_{forced}=\frac{1}{4\pi}\left(\sqrt{\gamma_M^2+4(1-\alpha)\omega_u^2}-\gamma_M\right)\left[\frac{V_s''+Y/L}{|V_u''|-Y/L}\right]^{1/2}e^{-Q/k_BT}, \tag{39}$$

which differs from (3) and (4) only by the appearance of the additional second-derivative contributions Y/L in both λ_+ and the R factor. To show that the same result emerges from the $\mu\rightarrow 0$ limit of Eq. (35) is not hard. The key is to notice that in this limit the solution for z occurs at $z\ll 1$, so that $\tanh z/z\approx 1$, and (35) reduces to $D(z)=\alpha$. The analog of (38) leads directly to (39).

C. Pure-polymer limit, $M=0$ (γM fixed)

In this limit, the trapped particle and its associated damping Γ_M both disappear; the end of the polymer is directly trapped but has no special mass of its own. The fact that β and $1/\omega_u$ both vanish as $M\rightarrow 0$ ($|V_u''|$ fixed) causes (35) to simplify to $\tanh z=\alpha z$ with solution $z(\alpha)$. The result is

$$\lambda_+^{(M=0)}=\tfrac{1}{2}\left(\sqrt{\gamma^2+4\omega_\mu^2 z^2(\alpha)}-\gamma\right), \tag{40}$$

which is similar in form to the Kramers result (4), except that the polymeric drag replaces γ_M. In particular, at small α (weak Y) $z(\alpha)\approx 1/\alpha$, so

$$\lambda_+^{(M=0)}\approx\frac{1}{2}\left(\sqrt{\left(\frac{L\Gamma}{L\mu}\right)^2+4\frac{|V_u''|}{\alpha L\mu}}-\frac{L\Gamma}{L\mu}\right), \tag{41}$$

where $\Gamma\equiv\mu\gamma$ is the polymeric drag per unit length. Equation (41) looks like (4) except that the particle mass M is replaced by the polymeric mass $L\mu$, the particle drag Γ_M is replaced by the net polymeric drag $L\Gamma$, and an extra factor α appears multiplying $L\mu$ in the denominator of the $|V_u''|$ term, thus enhancing the effective barrier frequency. The physical reason for this is that, for small Y, only a small fraction of the overall polymer contributes to the inertial mass associated with the binding site.

IV. RESULTS

With these limits now under control, we address the central issue: How does the polymer dynamics affect the Kramers escape? In this section we explore the effect of polymeric damping and mass on the escape rate on the basis of the general results (28) and (35). Our expectations here are not transparent, since increasing drag (which might be expected to slow escape) always comes with increasing noise (which might be expected to speed it up), because of Eq. (21). Experience with the forced-Kramers limit (and with the original Kramers problem) does lead us to expect a decrease of escape rate as overall damping is increased.

In this discussion, we focus on the net drag coefficients Γ_M and $L\Gamma$ for the particle and the polymer, respectively. A central question is the relative effectiveness of these two sources of frictional drag. In this connection it is convenient to define a nominal total drag

$$\Gamma_0\equiv\Gamma_M+L\Gamma, \tag{42}$$

$$\text{with } \Gamma_M=(1-\rho)\Gamma_0 \quad\text{and}\quad L\Gamma=\rho\Gamma_0, \tag{43}$$

so that the dimensionless parameter ρ ($0\leqslant\rho\leqslant 1$) determines what proportion of the total belongs to the polymer. By varying ρ, we can pass smoothly between the forced-Kramers case ($\rho=0$, Sec. III B), where all the drag attaches to the mass M, and the opposite extreme, $\rho=1$, where all the drag belongs to the polymer. When we need to express drag in dimensionless units, we shall write

$$g\equiv\frac{\Gamma_0}{M\omega_u}=\frac{\Gamma_0}{\sqrt{M|V_u''|}}\quad\text{or (when } M=0)$$

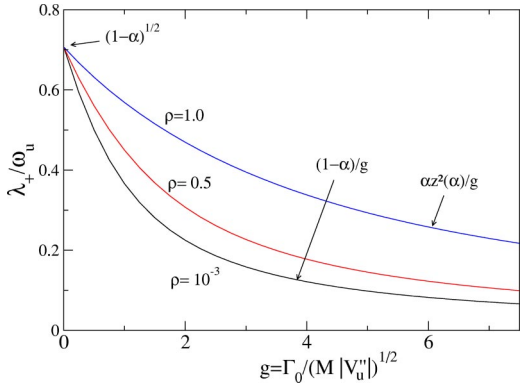

FIG. 3. The escape-rate prefactor λ_+/ω_u as function of g and ρ for $\mu=0$ (vanishing polymeric mass) and $\alpha=1/2$. g measures the overall drag [see Eqs. (42) and (44)], while ρ is the fraction of the overall drag due to the polymer [Eq. (43)]. At strong damping the escape rate falls off as $1/g$. The dependence of certain asymptotic limits on α is indicated on the plot.

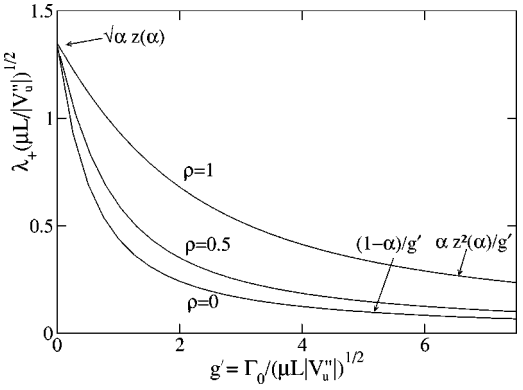

FIG. 4. The escape-rate prefactor as a function of g' [Eq. (44)] and ρ for $M=0$ (vanishing particle mass) and $\alpha=1/2$. The plot is similar to Fig. 3 except that the escape rate λ_+ and the overall drag Γ_0 have been made dimensionless by factors which do not involve M. At large g' the escape rate falls off as $1/g'$. The dependence of certain asymptotic limits on α is indicated in the plot.

$$g' \equiv g\sqrt{\beta} = \frac{\Gamma_0}{\sqrt{L\mu|V_u''|}}. \tag{44}$$

A. Distribution of drag between the trapped mass M and the polymer

A simple starting point is the case $\mu \to 0$, but now (in contrast to Sec. III B) with $\Gamma \equiv \gamma\mu$ fixed, so that the polymeric mass vanishes but its dissipation persists and can augment the effect of the direct drag Γ_M. This case will let us explore, in a particularly simple form the relative effects of frictional drag associated with the mass M and frictional drag associated with the polymer. In terms of the variables (42)–(44), Eqs. (28) and (35) for $\mu \to 0$ take the form

$$\frac{\lambda_+}{\omega_u} = \frac{\alpha}{\rho g} z^2(\alpha,\rho,g), \tag{45}$$

where $z(\alpha,\rho,g)$ is the unique positive solution of

$$\frac{\tanh z}{z} = \frac{\alpha}{1-(1-\rho)\dfrac{\alpha z^2}{\rho} - \left(\dfrac{\alpha z^2}{\rho g}\right)^2}. \tag{46}$$

At $\rho=0$, the result reduces to Eq. (39) with $\gamma_M/\omega_u = g$, so λ_+/ω_u goes to $\sqrt{1-\alpha}$ and $(1-\alpha)/g$ at $g=0$ and $g\to\infty$, respectively. At $\rho=1$, we find $\lambda_+/\omega_u = \sqrt{(1-\alpha)}$ and $\alpha z^2(\alpha)/g$ at $g=0$ and $g\to\infty$, respectively, where $z(\alpha)$ solves $\tanh z = \alpha z$. Figure 3 plots results for a range of values of g and ρ at $\alpha=1/2$ (other α values lead to qualitatively similar results). Note how increasing the overall friction g lowers the escape rate, just as for the original Kramers problem (3). At fixed overall drag g the escape rate is always increased by increasing ρ, i.e., by shifting drag from the mass M to the polymer. At strong damping the escape rate falls off as $1/g$. The coefficient of the $1/g$ behavior decreases monotonically from $\alpha z^2(\alpha)$ at $\rho=1$ to $(1-\alpha)$ at $\rho=0$.

Results similar to the above but for $M=0$, $\mu\neq 0$ and for $M=\mu L$ ($\beta=1$) are shown in Figs. 4 and 5, respectively. Generally speaking, what these calculations show is that polymeric friction is an important contributor to the total drag. Increasing the net drag always decreases the escape rate; however, drag exerted by the polymer is always less effective than the same net drag applied directly to M (see more in Sec. IV C).

B. Effect of the mass ratio

Next, we explore the effect of the mass ratio $\beta^{-1} = \mu L/M$. To separate this from drag effects, we start with the case $\gamma=0$ ($L\Gamma=0$), so that all the drag attaches to the trapped mass M. Figure 6(a) shows that increasing the polymeric mass at fixed drag always decreases the escape rate. Based on the Kramers problem, we expect mass effects to disappear at strong damping, and, indeed, a short calculation gives $\lambda_+ = (1-\alpha)\omega_u^2/\gamma_M = (1-\alpha)|V_u''|/\Gamma_M$, as $\gamma_M \to \infty$ for all values of β^{-1}. A nonzero polymeric friction does not change these qualitative trends. Figure 6(b) shows the escape rate as a function of damping when $\gamma=\gamma_M$ ($\Gamma_M = \beta L\Gamma$). We see the same decrease of escape rate as μL increases. In this case, the strong damping limit is $\lambda_+ = \alpha\beta z^2(\alpha)\omega_u^2/\gamma_M$ [$z(\alpha)$ solves $\tanh z = \alpha z$] as $\gamma_M \to \infty$. Note that, unlike the previous case,

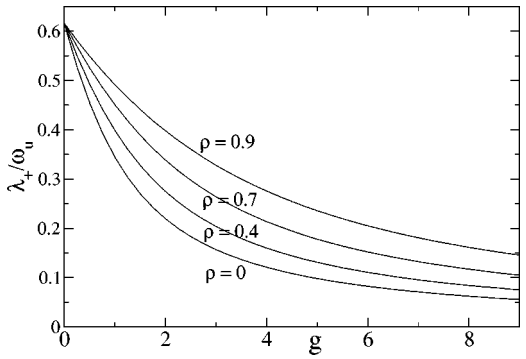

FIG. 5. Escape-rate prefactor as a function of g and ρ for $M=L\mu$ ($\beta=1$) and $\alpha=1/2$.

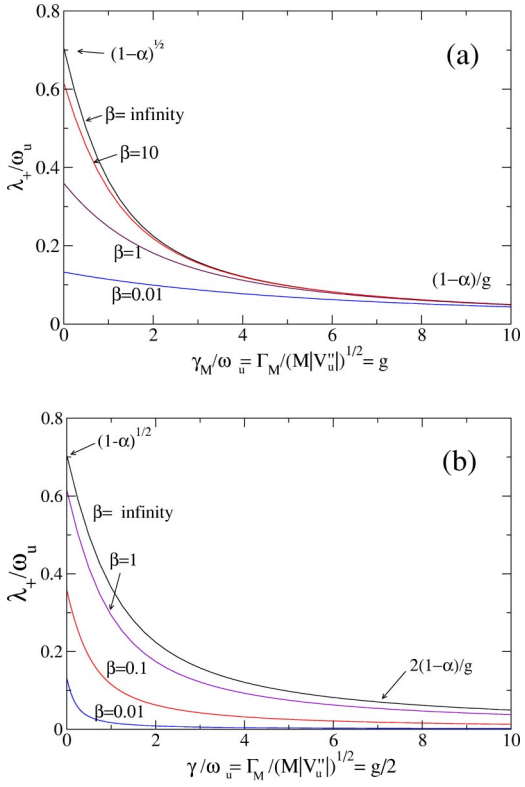

FIG. 6. Escape rate prefactor λ_+/ω_u as a function of g for $\alpha=1/2$ and several different values of $\beta^{-1}=L\mu/M$ to illustrate the effect of increasing polymeric mass. Part (a) treats the case of vanishing polymeric drag $\gamma=0$, while in part (b) we have taken $\gamma=\gamma M$ [see Eq. (37)]. Note that in all cases increasing the polymeric mass decreases the escape rate. The dependence of certain asymptotic limits on α is indicated in the plots.

there is here an explicit dependence on β in the strong-damping limit, which may be interpreted as a dependence of the effective friction on the mass ratio (see below).

C. Strong-damping limit

We conclude this section with a general discussion of strong damping, a situation which occurs commonly in biophysical applications and which we shall touch upon again in Sec. V C. We have seen that strong damping means slow escape, as in the original Kramers problem. In this limit the λ_+^2 terms in both Eqs. (27) and (29) may be dropped, and it is easy to show generally that

$$\frac{\lambda_+}{\omega_u}=\alpha\beta z^2\frac{\omega_u}{\gamma} \quad \text{with} \quad \frac{\tanh z}{z}=\frac{\alpha}{1-\dfrac{\gamma_M}{\gamma}\alpha\beta z^2}. \tag{47}$$

This is self-consistent, provided that $\lambda_+/\omega_u \ll \gamma/\omega_u$ in (27) and $\lambda_+/\omega_u \ll 1$ in (29). Both these conditions are satisfied whenever $\alpha\beta z^2 \ll \gamma/\omega_u$. We show below that this condition can always be satisfied provided the total drag $\Gamma_0 \equiv \Gamma_M + L\Gamma$ is sufficiently large; thus, Eq. (47) captures the entire strong-damping limit.

It is convenient to rewrite Eq. (47) in terms of the ρ,Γ_0 variables. Thus $(\gamma_M/\gamma)\alpha\beta=\alpha(\Gamma_M/L\Gamma)=\alpha(1-\rho)/\rho$, so $z=z(\alpha,\rho)$ in the hyperbolic tangent equation is a function of α and ρ but independent of the mass ratio β. Furthermore

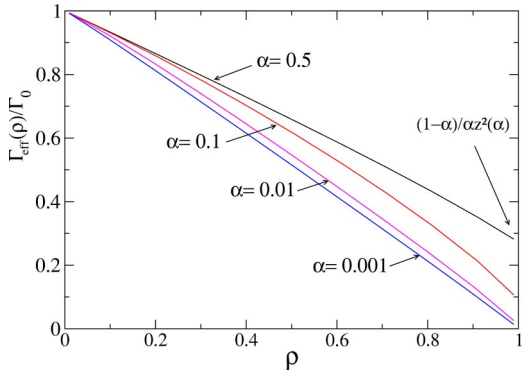

FIG. 7. Effective drag in the strong-damping limit for various values of α. In this limit, the escape-rate prefactor λ_+ always goes to zero with increasing total drag as $1/\Gamma_0$ [Eq. (48)] and the mass terms drop out of the Langevin equations (20). $\Gamma_{eff}(\rho)$ measures the effective drag which an isolated mass M would need to have in order to achieve the same escape rate as it does in the presence of the polymer. The decrease of Γ_{eff} as ρ increases reflects the reduced effectiveness of the polymeric drag compared to the particle drag. At $\alpha=0$ the polymer decouples completely from the escape, so $\Gamma_{eff}=\Gamma_M=(1-\rho)\Gamma_0$.

$$\lambda_+=\alpha\beta z^2(\alpha,\rho)\frac{\omega_u^2}{\gamma}=\frac{\alpha z^2(\alpha,\rho)|V_u''|}{\rho\Gamma_0}. \tag{48}$$

The result that the escape rate is independent of the masses at strong damping is not unexpected, since the inertial terms in the Langevin equations (20) drop out in this limit.

We return now to the issue of self-consistency. Recall that $z(>0)$ can be small but is bounded above by $1/\alpha$. Thus, λ_+ can be made arbitrarily small, provided only that $\rho\neq 0$ (i.e., that $\gamma\neq 0$). But, as $\rho\to 0$, z becomes small, the left side of the hyperbolic tangent equation approaches unity, and we find $\alpha z^2/\rho=(1-\alpha)$ or $\lambda_+(\rho=0)=(1-\alpha)|V_u''|/\Gamma_0$, as we have already found in Sec. IV A. Thus, the $\rho=0$ limit is not singular, and λ_+ can always be made small by taking Γ_0 large.

Comparison with the forced-Kramers limit $\rho=0$ suggests that we write the strong-damping result (47) in terms of an effective drag

$$\lambda_+\equiv\frac{(1-\alpha)|V_u''|}{\Gamma_{eff}(\alpha,\rho)}, \tag{49}$$

where Γ_{eff} is the drag coefficient that would have to be assigned to the mass M to simulate the effect of the polymeric drag in the strong-damping limit. Comparing Eqs. (48) and (49) leads to the evaluation

$$\frac{\Gamma_{eff}}{\Gamma_0}=\frac{(1-\alpha)\rho}{\alpha z^2(\alpha,\rho)}. \tag{50}$$

This function, which is independent of the mass ratio β, is plotted in Fig. 7 for a selection of α values. The fact that this function decreases from its limiting value of unity at $\rho=0$ indicates that the polymeric drag coefficient ΓL is less effective than Γ_M, as might be expected from the fact that, in the

unstable mode, the polymeric units move with lower velocity than the particle M. For example, a short calculation for small ρ shows that $\Gamma_{eff}(\rho)=\Gamma_0(1-2\rho/3+\cdots)\approx\Gamma_M+L\Gamma/3$, so that the effective drag coefficient for M is increased by the polymeric attachment, as expected, but not by the full amount $L\Gamma$. At larger values of ρ the curves depart from this simple linear relation, reflecting a more complex dependence on the ratio $\Gamma_M/L\Gamma$. As $\alpha\to 0$, the function $\Gamma_{eff}(\rho)$ approaches $\Gamma_0(1-\rho)=\Gamma_M$. This is not surprising, since $\alpha=0$ is the Kramers limit (Sec. III A), where the polymer decouples from the particle, so polymeric drag is completely ineffective.

V. DISCUSSION AND CONCLUSIONS

A. Comparison to previous theoretical work

Multibody escape problems with a flavor similar to ours have been addressed by Sebastian and Puthur [14]. These authors calculated the rate of thermally assisted breakage of a bond in the middle of a chain by applying multidimensional transition state theory. Transition state theory (TST) [12] starts from the equilibrium partition function and calculates the overall outflux from the trap, neglecting recrossing events back into the trap. It cannot take into account the effect of friction on the dynamics near the trap, so the role of friction (and noise) is seen only in setting up the equilibrium ensemble. Thus, TST typically overestimates the rate, as is well documented in the literature [12]. The Kramers formalism, on the other hand, computes the net outward flux across the barrier from the true nonequlibrium phase-space probability density obtained by solving the Fokker-Planck equation of the corresponding Langevin equation. In Ref. [14], the authors try to put back the missing effect of friction by cooking up a special harmonic bath, because it is known that the Kramers' result can be obtained from TST for a single particle if the particle is quadratically coupled to a harmonic bath. Then, the simple Kramers formula emerges in some special limit. The applicability of such a scheme to the multibody case has not been proved. In Kramers-Langer formalism, which we use, no such *ad hoc* modeling is required to incorporate the effect of friction.

B. Weak-damping limit

The Kramers calculation in the form used here fails in the weak-damping limit, as was noted in the original article [1]. The reason for this failure is that, in the derivation, it is assumed that the distribution in the barrier region can be fit to a stationary, quasiequilibrium distribution inside the well. When a weakly damped particle undergoes a complete oscillation inside the well and returns to the barrier region without appreciable energy loss, then this assumption breaks down because there are memory effects which cannot be ignored. Trajectories which suffer energy loss greater than k_BT do not return to the barrier region. Thus, the criterion that these memory effects can be neglected is simply that the energy loss in one cycle of the undamped mechanical motion should be greater than k_BT, which leads to the estimate Eq. (5) for the range of validity. To describe behavior outside this range, as $\gamma_M\to 0$, requires a different approach, usually based on the notion of energy (or action) diffusion [15].

It seems safe to state that a similar breakdown of the Langer derivation [9] for the many-particle case studied here should occur at weak coupling. And, indeed, Eq. (5) presumably provides a first estimate as to where this breakdown may be expected to occur. Although it would be interesting to explore this region more fully, such a study is beyond the scope of the present work. Nevertheless, it is interesting to note that the conclusion that the escape rate goes to zero at zero damping most likely does not hold in general for the many-particle system. The reason is that the polymeric degrees of freedom all have energies of order k_BT. Thus, for a polymer of appreciable length, the average energy of the system is many times k_BT, whereas, typically, the barrier height Q is only a few k_BT. Thus, there is plenty of energy available for the system to escape over the barrier even when no noise (and no dissipation) is present. In this limit, it would seem, escape becomes a problem in (nonlinear) dynamics.

C. Biophysical applicability of the model

Although motivated by the biophysical experiments referenced in Sec. I, the one-dimensional model proposed here is a significant simplification. Real polymeric linkers have significant short-range interactions, which are neglected here. Furthermore, at sufficiently low tensions F, Eq. (9), even without short-range interaction, a long polymer adopts a random-coil configuration rather than being linear, as assumed here. The model proposed here could only apply in the so-called "overstretched" regime, when the tension is strong enough to overcome entropic effects and force the polymer into a linear configuration. Luckily, this is sometimes the case in experiments [5,7,8]. Even in this situation there would be some corrections due to the out-of-line motion, although these may be expected to be small at high enough tension.

Another problem is the form of the drag coefficients. We have assumed that each "bead" has its own independent drag force. This assumption will break down when there are significant hydrodynamic interactions between beads. Even in the strictly linear situation envisaged here, the friction for individual spherical monomers (for example) will not typically translate additively into the frictional coefficient Γ per unit length of the polymer, since the flow pattern around individual beads is affected by close spacing, unless the beads are widely separated. These cooperative effects could be large for coiled configurations; however, for the linear case treated here, we expect them to be quantitative rather than qualitative.

The upshot is that we expect our calculations should be capable of giving a good account of qualitative issues for experiments in which the tension is strong enough to pull the polymer into an extended configuration.

D. Biophysical experiments

The objective of this section is to get an idea of representative values which the parameters in our theory might take in a typical experimental system. We imagine a strand of

DNA of length $L_0=1$ μm with one end attached to a fixed support and the other end in a kinetic trap. For simplicity we shall assume that the particle which feels the trapping potential is not significantly different in mass and drag from the DNA monomers, so we are in the regime $M=0$ and Eq. (40) applies. Each base pair has a mass of 660 daltons (D), so, using a linear density of one base pair per 0.34 nm ($\sim$1900 D/nm), we calculate a mass density $\mu\sim 3\times10^{-15}$ kg/m. In order for our one-dimensional model to have any hope of being applicable (see Sec. V C), it is necessary that the applied tension suffice to stretch out the thermal coil of the relaxed polymer into a nearly linear configuration. Experimentally, this occurs for $F\sim 1$ pN [16], which is consistent with the theoretical criterion that $F\gg k_BT/\xi_p \sim 8\times10^{-14}$ N [17], where $\xi_p\sim 53$ nm is the persistence length of DNA [18]. At the other extreme, the onset of DNA overstretching is observed at $F\sim 60$ pN [7,8]. In this window, 1 pN$<F<$60 pN, the stretching of the DNA backbone is relatively small, since $Y_0\sim 900$ pN [7], giving a fractional extension of no more than 7% by Eq. (9).

To decide whether we are in the overdamped or the underdamped regime, we need to estimate the parameters appearing in Eq. (40). The largest uncertainty comes from the factor $|V_u''|$. We estimate $|V_{u,s}''|\sim \Delta V/(\Delta x)^2$, where ΔV is the depth of the trap and Δx is a characteristic length scale associated with the trapping potential. Taking $\Delta V\sim 25k_BT$ and Δx between an angstrom and a nanometer puts $|V_u''|$ in the range 0.1–10 N/m, which gives $\alpha\sim 10^{-4}-10^{-2}$ from the definition (12). Finally, we estimate the drag as $\Gamma\sim 3\pi\eta \sim 10^{-2}$ Ns/m^2. The fact that $\alpha\ll 1$ means that we can use Eq. (41) in place of Eq. (40). The ratio which determines the degree of overdamping is

$$\frac{\gamma}{2\omega_\mu z(\alpha)}\sim\frac{\alpha\gamma}{2\omega_\mu}=\frac{1}{2}\frac{\Gamma}{|V_u''|}\sqrt{\frac{Y_0}{\mu}}, \tag{51}$$

which works out to be in the range 0.3 (for the angstrom-range trap) up to 30 (for the nanometer-range trap), indicating moderate to strong damping. The corresponding escape-rate prefactors range from $\lambda_+/2\pi\sim 2\times10^8-7\times10^{11}$ s^{-1}, with the lower value for the nanometer-scale trap. To estimate the full escape rate, it is necessary to provide values for the remaining factors in Eq. (30). Taking $R\sim 1$ and $Q\sim 20k_BT$ gives an escape rate $r\sim 0.4$–1500 s^{-1}, with the lower value for the nanometer-scale trap. These values encompass the range of typical bond-rupture experiments [19]. Of course, these numbers are very sensitive to the well depth Q. Every decrease of $5k_BT$ in well depth corresponds to an increase in escape rate by a factor of 150. In this connection, we note that applied tension can decrease the bare well depth significantly, Eqs. (6) and (32), as emphasized by Evans and Ritchie [4]: $F(L_s-L_u)\sim 1.5-15k_BT$ for a tension of $F\sim 60$ pN and a trap size of $(L_u-L_s)\sim 10^{-10}-10^{-9}$ m, respectively.

It is instructive to compare some of these numbers with what we would have found had we approximated the DNA problem above as a simple forced-Kramers escape, Eqs. (3), (6), and (39), treating the terminal polymeric unit as the mass M but neglecting the mass and drag of the remaining polymeric units, so that they only enter the problem as the agent for the applied tension F. The comparison is, then, between the correct prefactor (40) and the forced-Kramers approximation (4). The drag parts of these expressions are the same, since $\gamma_M=\gamma\sim 3\times10^{12}$ s^{-1} is the drag per unit mass. The difference comes in the trap term. The relevant comparison here is

$$\frac{\omega_\mu^2 z^2}{\omega_u^2}\sim\frac{\omega_\mu^2}{\alpha^2\omega_u^2}=\frac{M|V_u''|}{\mu Y_0}, \tag{52}$$

where we have used the small-α approximation. This ratio works out for the DNA problem to be in the range 0.03 (for a nanometer trap) to 3 (for an angstrom trap); it enters the prefactor λ_+ directly in the strong-damping limit or as a square root in the weak-damping limit. The upshot is that, for a nanometer trap, the forced-Kramers estimate of the escape rate is up to 30 times too fast in the strong-damping limit, although this discrepancy rapidly becomes smaller as the trap becomes stiffer. (Note, also, that the fact that $z\omega_\mu<\omega_u$ in this case means that $\gamma/z\omega_\mu>\gamma_M/\omega_u$, so the escape-rate prefactor is further towards the strong-damping regime than the forced-Kramers approximation would indicate.) At first sight, it may seem accidental that the combination of factors on the right side of Eq. (52) is so close to unity, i.e., that the forced-Kramers approximation is so good. To understand why, we note that M/μ is a length of order the monomer diameter; $|V''|$ is comparable to K_1 in Eq. (13); and, $Y_0=ka$ from Eq. (9). Thus, if a is comparable to the monomer size, we find that $\omega_\mu^2 z^2/\omega_u^2\sim K_1/k$, i.e., the ratio of the trap stiffness to the stiffness of the polymeric links. If these two stiffnesses are comparable, which is not unusual, the forced-Kramers approximation is never too bad (at least, as long as α is small).

So far, all our estimates have been for DNA, which is a relatively light biopolymer. How do these numbers change for heavier polymers? The key ratio (at small α) is $\alpha\gamma/\omega_\mu=(\Gamma/|V_u''|)\sqrt{(Y_0/\mu)}$. Only the square-root factor is dependent on polymer properties. It turns out that this factor is only weakly dependent on the polymer mass density. The reason is that $Y_0\sim\pi R^2 Y^{(3D)}$, where $Y^{(3D)}$ is the three-dimensional modulus and R is the polymeric radius [18]. Furthermore, $\mu\sim\pi R^2\rho$, where ρ is the density of the bulk polymeric material. It follows that $Y_0/\mu\sim Y^{(3D)}/\rho$. For many biopolymers $Y^{(3D)}=(0.5-1.5)\times10^9$ N/m^2 and $\rho\sim\rho_{water}$, and the ratio (Y_0/μ) changes by less than a factor of 10 for polymers ranging in linear mass density by a factor of 10^5 [18]. There seems to be a weak trend for heavier polymers to have larger $Y^{(3D)}$, putting them further toward the strong-damping regime.

We are not aware of any extant experiments to which our model might be directly applied. Nevertheless, there are experiments on the muscle protein titin [5] and polysaccharides [6] to which our considerations apply, albeit in somewhat altered form. We take the example of titin [5], which consists of a linear sequence of immunoglobulin (Ig) domains connected by deformable proline-, glutamate-, valine-, and lysine-rich (PEVK) segments. The Ig domains are globular; but, under sufficient tension they unfold into an over-

stretched configuration by breaking internal hydrogen bonds. The PEVK segments act like flexible springs. As the overall tension applied to the polymer is increased beyond the unfolding threshold, the Ig domains unfold one by one, producing a sawtooth shape in the observed force-extension curve. If the applied force were held constant [20], then each individual unfolding event would be similar to our model, except that the breakage point is at some point in the middle of the polymer segment rather than at one end. Thus, in considering each event, it is in principle necessary to consider not only the mass and drag of the breaking Ig domain but the full mass and drag of all parts of the polymer. The inertial effects of the mass are likely irrelevant, since the system is probably in an overdamped regime. Nevertheless, as we have shown herein, there can still be significant effects on the escape-rate prefactor arising from drag forces away from the breakage site.

E. Conclusions

We have shown that the forced-Kramers escape rate can be significantly altered by the properties of the polymeric spring. In general, coupling of the dynamical degrees of freedom of the polymer to those of the escaping particle leads to changes in the prefactor of the escape rate (the effective attempt rate) which cannot be captured by simply assigning an effective mass and drag to the escaping particle. The reason for this is that the dynamics, itself, controls how much of the mass and drag of the polymer should be associated with the escape. In the strong-damping limit, the mass terms disappear from the Langevin equations and an effective drag can be defined. However, even in this case the effective drag is not simply additive [see Eq. (50) and Fig. 7]. Increasing the polymeric mass always decreases the escape rate, as does increasing the overall drag; however, a shift of drag from the trapped particle to the polymer increases the escape rate.

Although we have treated the case of a one-dimensional polymeric spring, it is clear that similar effects will occur whenever other dynamical degrees of freedom are coupled to a simple trap. (For example, one might consider a trap coupled to a fluctuating membrane.) The additional degrees of freedom act as a kind of structured bath, which interacts with and modifies the effects of the unstructured thermal bath. The Langer [9] formalism serves as an elegant tool for capturing these effects, provided that the damping is not too weak.

ACKNOWLEDGMENTS

We are grateful to Evan Evans for stimulating our interest in this problem. A.S. would like to thank K. L. Sebastian for pointing out his work on polymer breakage problems. This work was supported in part by the Natural Sciences and Engineering Research Council of Canada.

APPENDIX: CALCULATION OF R IN EQ. (31)

The $(N+1)\times(N+1)$-dimensional matrices $\mathbf{E_2}^{(s,u)}$ in Eq. (31) have the tridiagonal structure

$$\begin{pmatrix} 1-C_{s,u} & -1 & 0 & \dots & 0 \\ -1 & 2 & -1 & 0 & \vdots \\ 0 & -1 & 2 & -1 & \vdots \\ \vdots & 0 & -1 & \ddots & -1 \\ 0 & \dots & 0 & -1 & 2 \end{pmatrix}, \tag{A1}$$

where $C_{s,u}=-V''_{s,u}/k$ and $V''_{s,u}$ was, e.g., given for the cubic potential in Eq. (16). The determinant of this matrix can be evaluated directly

$$\det \mathbf{E_2}^{(s,u)} = 1 - C_{s,u}(N+1). \tag{A2}$$

In this evaluation, we have used the fact that the determinant of the $N\times N$-dimensional matrix which arises by striking out the first row and column of Eq. (A1) is equal to $(N+1)$. This matrix occurs in the treatment of phonons in a harmonic chain of N masses with the ends held fixed.

The matrix E_2 can at most have one negative eigenvalue, i.e., one unstable mode. The condition for the existence of such a mode is that $\det \mathbf{E}_2<0$. This can only be satisfied at the unstable equilibrium $(V''_u<0)$, when $1<(N+1)C_u$. This condition is equivalent by virtue of Eqs. (10) and (24) to $\alpha<1$, Eq. (12), which in turn is related to the existence of the unstable continuum mode discussed after Eq. (35).

[1] H.A. Kramers, Physica (Utrecht) **7**, 284 (1940).
[2] The strict low-damping limit is not achieved, since it is preempted by the condition $\gamma_M>\omega_s(k_BT/Q)$, below which the true escape rate does not obey Eq. (3) but goes smoothly to zero [1]. However, the escape rate can approach the low-damping limit before this turnover because, typically, $\omega_s\sim\omega_u$ and $k_BT/Q\ll 1$.
[3] G.I. Bell, Science **200**, 618 (1978).
[4] E. Evans and K. Ritchie, Biophys. J. **72**, 1541 (1997).
[5] L. Tskhovrebova, J. Trinick, J.A. Sleep, and R.M. Simmons, Nature (London) **387**, 308 (1997);M.S. Z. Kellermayer, S.B. Smith, H.L. Granzier, and C. Bustamante, Science **276**, 1112 (1997);M. Rief, M. Gautel, F. Oesterhelt, J.M. Fernandez, and H.E. Gaub, *ibid.* **276**, 1109 (1997).
[6] M. Rief, F. Oesterhelt, B. Heymann, and H.E. Gaub, Science **275**, 1295 (1997); M. Rief, J.M. Fernandez, and H.E. Gaub, Phys. Rev. Lett. **81**, 4764 (1998).
[7] J.F. Marko, Phys. Rev. E **57**, 2134 (1998).
[8] I. Rouzina and V.A. Bloomfield, Biophys. J. **80**, 882 (2001).
[9] J. Langer, Ann. Phys. (N.Y.) **54**, 258 (1969).
[10] H. Risken, *The Fokker-Planck Equation* (Springer-Verlag, Berlin, 1984), p. 88. Risken discusses the derivation of the Fokker-Planck equation from the Langevin equation. The result cited is for two coupled particles but is easily generalizable. It is straightforward to show that this Fokker-Planck

equation leads at long time to thermal equilibrium at temperature T.

[11] The dropping of the noise term in arriving at Eqs. (28) and (29), which define λ_+, might make it appear that noise has been neglected in arriving at the Langer escape rate (30). This is not so, as examination of the full derivation [9,12] makes clear. To see how this works out for the ordinary Kramers case, the reader is invited to set $Y=0$ ($k=0$) in Eqs. (22) and (23). This leads to the equation $\lambda_+^2+\gamma_M\lambda_+-\omega_u^2=0$, the positive root of which is just λ_+^{Kr}, Eq. (4). See also Sec. III A.

[12] P. Hänggi, P. Talkner, and M. Borkovec, Rev. Mod. Phys. **62**, 251 (1990).

[13] Of course, when Q becomes comparable to k_BT, then escape begins to depend on initial conditions (injection) and the Kramers formula fails as in Eq. (5). We assume that $Q\gg k_BT$, so that Eq. (34) is valid.

[14] K.L. Sebastian and R. Puthur, Chem. Phys. Lett. **304**, 399 (1999); Phys. Rev. B **66**, 024304 (2002).

[15] Further references and discussion of this point are given in Hänggi [12]. For the one-particle Kramers problem, the result is an escape rate which vanishes linearly with γ_M as $\gamma_M\rightarrow 0$, reflecting the fact that, when there is no dissipation, there is no noise, so simple energy conservation prevents all escape.

[16] C. Bouchiat, M.D. Wang, J.-F. Allemand, T. Strick, S.M. Block, and V. Croquette, Biophys. J. **76**, 409 (1999).

[17] J.F. Marko and E.D. Siggia, Macromolecules **27**, 981 (1995).

[18] D. Boal, *Mechanics of the Cell* (Cambridge University Press, Cambridge, 2002). The linear mass densities (D/nm) and persistence lengths ξ_p for different polymers are tabulated in Chap. 2.

[19] E. Evans and K. Ritchie, Biophys. J. **76**, 2439 (1999).

[20] In the actual experiments [5], the tension is not held fixed but, rather, it is ramped up between breakage events. In this situation the average breakage force depends significantly on the ramping rate, as has been discussed by Evans and Ritchie [4], and the Kramers formula (upon which our manuscript is focused) is only the starting point of the calculation. Evans and Ritchie [19] have carried out a partial analysis of the problem, including the ramping but ignoring the mass and drag of the polymeric degrees of freedom.